PHYSICAL REVIEW D **96,** 075046 (2017)

# Impact of LHC data on muon $g-2$ solutions in a vectorlike extension of the constrained MSSM

Arghya Choudhury,[1,*] Soumya Rao,[2,†] and Leszek Roszkowski[1,2,‡]

[1]*Consortium for Fundamental Physics, Department of Physics and Astronomy, University of Sheffield, Sheffield S3 7RH, United Kingdom*

[2]*National Centre for Nuclear Research, Hoża 69, 00-681 Warsaw, Poland*

(Received 6 September 2017; published 31 October 2017)

The long-standing discrepancy between the experimental determination by the Muon $g-2$ Collaboration at Brookhaven and the Standard Model predictions for the anomalous magnetic moment of the muon cannot be explained within a simple unified framework like the constrained minimal supersymmetric standard model, but it can within its extension with vectorlike fermions. In this paper we consider a model with an additional vectorlike $5+\bar{5}$ pair of $SU(5)$. Within this model we first identify its parameter space that is consistent with the current discrepancy and show that this implies the lighter chargino mass in the range of 700–1200 GeV. We examine how it is affected by constraints from the electroweak sparticle search at the LHC based on a 13 TeV search with 36.1 fb$^{-1}$ integrated luminosity. We show that null trilepton signal searches coming from chargino-neutralino pair production significantly constrain the allowed parameter space except when the chargino-neutralino mass difference is relatively small, below about 10 GeV. Next we consider the expected impact of the New Muon $g-2$ experiment at Fermilab with its projected sensitivity reach of $7\sigma$ and, assuming it confirms the current discrepancy, show that the remaining parameter space of the considered model will be in strong tension with the current LHC limits.

DOI: 10.1103/PhysRevD.96.075046

## I. INTRODUCTION

Despite the absence of a signal for supersymmetry (SUSY) at the LHC, it still remains one of the most appealing frameworks for physics beyond the Standard Model (BSM). Besides providing a natural candidate for dark matter (DM), it also gives a possible explanation for the discrepancy that exists in the Standard Model (SM) value of the anomalous magnetic moment of muon, $(g-2)_\mu$, and the experimentally measured quantity. The SM value for $(g-2)_\mu$ differs by more than $3\sigma$ from the measured value [1,2]. Future measurement at Fermilab [3,4] is expected to improve the sensitivity of the previous measurement by a factor of 4 and hence potentially confirm or falsify the persistent disagreement. In SUSY, the explanation for the difference arises from contributions due to smuon-neutralino and sneutrino-chargino loops. To fit the $(g-2)_\mu$ anomaly within the framework of the minimal supersymmetric Standard Model (MSSM), one requires the slepton and the lighter chargino masses in a range of a few hundreds of GeV [5–11]. However, the stringent bounds on the strong sector (squarks and gluinos) from the LHC and the Higgs mass measurements rule out the possibility of explaining $(g-2)_\mu$ in Grand Unified Theory (GUT)-constrained models such as the constrained MSSM (CMSSM) and the nonuniversal Higgs Mass (NUHM) model [12–14]. The way out has usually been to assume nonuniversal gaugino masses [15–22] which can provide a viable parameter space to explain $(g-2)_\mu$ while at the same time not conflicting with constraints from LEP and LHC.

There have also been alternative solutions as, for example, adding vectorlike (VL) matter to MSSM which has been studied in Refs. [23–32]. The presence of a new VL sector gives an extra contribution to $(g-2)_\mu$ by introducing new sources of smuon mixing and new Yukawa couplings [32]. Apart from $(g-2)_\mu$, it has been shown that VL colored sparticles provide extra contributions to the Higgs mass [33–38], and several phenomenological analyses have addressed the extra VL matter in the context of various long-standing theoretical issues related to beyond SM physics [23–32].

In particular, Ref. [32] studied two simple extensions of the CMSSM by adding a pair of multiplets, first in the $\mathbf{5}+\bar{\mathbf{5}}$ and second in the $\mathbf{10}+\overline{\mathbf{10}}$ representations of $SU(5)$. It was shown that the model could satisfy various constraints from flavor physics and LHC direct searches, as well as include a viable dark matter candidate that was in agreement with relic density and direct detection constraints, for a considerable region of the parameter space [32]. In particular, through the additional mixing of VL fields with second generation leptons, the model proved particularly useful in explaining the $(g-2)_\mu$ discrepancy. In this work we extend the analysis considered in Ref. [32], using the models with additional $\mathbf{5}+\bar{\mathbf{5}}$. Motivated by the

*a.choudhury@sheffield.ac.uk
†soumya.rao@ncbj.gov.pl
‡leszek.roszkowski@ncbj.gov.pl

 

solution to the $(g-2)_\mu$ discrepancy, we examine the impact of collider constraints on the viable parameter space.

As mentioned earlier, the allowed parameter spaces satisfying $(g-2)_\mu$ constraints are characterized by light electroweak (EW) sparticles, i.e., light EW gauginos or electroweakinos (the charginos and the neutralinos) and charged sleptons. Hence, to probe the relevant parameter space at the LHC, the most sensitive search is chargino and neutralino pair production (via $pp \to \chi_1^\pm \chi_2^0$) leading to the trilepton + transverse missing energy ($\not{E}_T$) signal. Both CMS and ATLAS Collaborations have looked for electroweakinos, or EWinos, with different leptonic final states [39–47], among which the trilepton data give the most stringent bound. From the very recent LHC analysis of Run-II data with $\mathcal{L} = 36.1$ fb$^{-1}$, ATLAS has excluded chargino masses up to 1150 GeV for relatively light lightest supersymmetric particle (LSP) [46]. However, ATLAS and CMS have presented these limits for a few particular types of simplified models with specific assumptions on the compositions and branching ratios of EWinos. The electroweakinos searches and related topics in the context of the LHC have been analyzed by various phenomenology groups in Refs. [7,9,48–66]. Because of the presence of VL particles and their mixing with SM, the electroweakinos (mainly $\chi_1^\pm, \chi_2^0$) can have nonstandard branching ratios compared to the CMSSM or usual phenomenological MSSM (pMSSM) scenarios. Hence the limits interpreted by ATLAS or CMS for various simplified models are not directly applicable to such models and a reinterpretation of the bounds from trilepton searches at the LHC is necessary.

The paper is organized as follows. We first give a brief overview of the model which is obtained by adding a VL $\mathbf{5}+\bar{\mathbf{5}}$ of $SU(5)$ pair to CMSSM in Sec. II. We briefly mention the constraints applied to obtain the relevant allowed parameter space in Sec. III and then discuss different scenarios for chargino ($\chi_1^\pm$) and neutralino ($\chi_2^0$) decays in the context of a VL extension of CMSSM in Sec. IV. In Sec. V, we show results for LHC trilepton searches from chargino-neutralino pair production using the latest LHC Run-II 36.1 fb$^{-1}$ data. Finally, we give our conclusions in Sec. VI.

## II. VECTORLIKE EXTENSION OF THE CMSSM

We follow the model studied and analyzed in [32], particularly in the context of $(g-2)_\mu$ where the MSSM is extended through the addition of a pair $\mathbf{5}+\bar{\mathbf{5}}$ or a pair $\mathbf{10}+\overline{\mathbf{10}}$. However, it was shown in [32] that the $\mathbf{10}+\overline{\mathbf{10}}$ extension was more fine-tuned in order to provide a viable parameter space for a significant contribution to $(g-2)_\mu$, and therefore the analysis was restricted to $\mathbf{5}+\bar{\mathbf{5}}$. Here we shall focus only on the $\mathbf{5}+\bar{\mathbf{5}}$ extension, which from now on we shall refer to as the LD model following the previous convention. We summarize the main features of the LD model below (for more details see Ref. [32]).

The LD model consists of extending the MSSM spectrum with the addition of the following fields[1]:

$$D = (\bar{\mathbf{3}}, \mathbf{1}, 1/3), \qquad D' = (\mathbf{3}, \mathbf{1}, -1/3),$$
$$L = (\mathbf{1}, \mathbf{2}, -1/2), \qquad L' = (\mathbf{1}, \mathbf{2}, 1/2).$$

This implies the addition of a quark with charge $-1/3$ and a charged lepton along with their antiparticles, and two massive neutrinos to the MSSM spectrum. Correspondingly the sparticle content sees the addition of squarks, sleptons, and sneutrinos.

In comparison to the MSSM, there are now additional trilinear and bilinear terms in the superpotential,

$$W \supset -\lambda_D q H_d D - \lambda_L L H_d e + M_D D D' + M_L L L' + \tilde{M}_L l L' + \tilde{M}_D d D'. \tag{2.1}$$

Finally the soft SUSY-breaking Lagrangian also has extra terms involving $\tilde{L}^{(\prime)}$ and $\tilde{D}^{(\prime)}$ as follows:

$$\begin{aligned} -\mathcal{L}_{\text{soft}} \supset\ & [m_L^2 |\tilde{L}|^2 + m_{L'}^2 |\tilde{L}'|^2 + m_D^2 |\tilde{D}|^2 + m_{D'}^2 |\tilde{D}'|^2 \\ & + (\tilde{m}_L^2 \tilde{l}^\dagger \tilde{L} + \tilde{m}_D^2 \tilde{d}^\dagger \tilde{D} + \text{H.c.})] \\ & + (B_{M_L} \tilde{L}\tilde{L}' + B_{\tilde{M}_L} \tilde{l}\tilde{L}' + B_{M_D} \tilde{D}\tilde{D}' \\ & + B_{\tilde{M}_D} \tilde{d}\tilde{D}' + \text{H.c.}) \\ & - (T_D \tilde{q} H_d \tilde{D}^\dagger + T_L \tilde{L} H_d \tilde{e}^\dagger + \text{H.c.}), \end{aligned} \tag{2.2}$$

where $\tilde{m}_L^2$, $\tilde{m}_D^2$, $T_L$, $T_D$, $B_{\tilde{M}_L}$, and $B_{\tilde{M}_D}$ are three-dimensional matrices that govern mixing between MSSM and VL matter. This mixing plays an important role for $(g-2)_\mu$ phenomenology.

In addition to the above, we also make the choice of GUT scale parameters such that the boundary conditions for the extra Yukawa couplings demanded by UV completion at the GUT scale are given by

$$\lambda_L = \begin{pmatrix} 0 \\ \lambda_5 \\ \epsilon\lambda_5 \end{pmatrix}, \tag{2.3}$$

where $\epsilon < 1$. This in turn means that the soft mass matrices, which also satisfy the same flavor constraints as the Yukawa couplings, will have their off-diagonal mixing terms parametrized similar to Eq. (2.3) as follows:

$$\tilde{m}_L^2 = \tilde{m}_D^2 = \begin{pmatrix} 0 \\ \tilde{m}^2 \\ \alpha\tilde{m}^2 \end{pmatrix}, \tag{2.4}$$

where once again $\alpha < 1$.

[1]The MSSM fields are $q = (3, 2, 1/6)$, $u = (\bar{3}, 1, -2/3)$, $d = (\bar{3}, 1, 1/3)$, $l = (\mathbf{1}, \mathbf{2}, -1/2)$, $e = (\mathbf{1}, \mathbf{2}, -1/2)$, $H_u = (1, 2, 1/2)$, $H_d = (1, 2, -1/2)$ with $SU(3) \times SU(2) \times U(1)$ quantum numbers in parentheses.

Thus the first generation mixing is almost absent compared to second and third generation mixing. Equations (2.3) and (2.4) not only impact the $(g-2)_\mu$ contribution but also have a significant effect on the trilepton signal from chargino and neutralino decays as we shall see in Sec. IV.

## III. CONSTRAINTS FROM FLAVOR PHYSICS, $(g-2)_\mu$, AND DIRECT DETECTION OF DM

In this section we mention the GUT scale input parameters used as well as the constraints applied in order to obtain the parameter space shown in Fig. 1.[2] The parameter space was scanned using MULTINEST [67], and the SARAH [68–71] package was used to generate the spectrum, while the relevant flavor constraints were calculated using the SARAH package FLAVORKIT [72]. In addition, dark matter constraints on relic density and direct detection were obtained using MICROMEGAS v.3.5.5 [73]. Bounds on the Higgs sector from LHC searches for Higgs production channels, branching ratios as well as Higgs decay were applied using the codes HIGGSSIGNALS [74] and HIGGSBOUNDS [75–77]. The following ranges of values for the GUT scale input parameters were used, which are also listed in [32]:

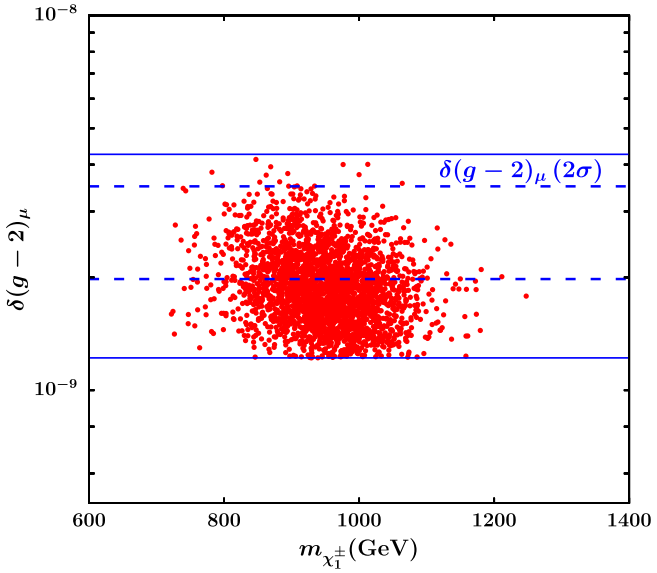


FIG. 1. Allowed parameter space for $\delta(g-2)_\mu$ in the LD model as a function of chargino mass. The $2\sigma$ allowed region for $\delta(g-2)_\mu$ according to the latest data [1,2] is indicated by the blue solid lines, while the dashed lines indicate future measurement [3,4] with 4 times greater sensitivity, assuming that the central value remains the same.

$$
\begin{aligned}
\text{VL Yukawa coupling,} &\quad \lambda_5 \in [-0.5, 0.5],\\
\text{Yukawa hierarchy factor,} &\quad \epsilon \in [-0.5, 0.5],\\
\text{superpotential mass VL fields,} &\quad M_V \in [50, 1500]\ \text{GeV},\\
\text{superpotential mass mixing,} &\quad \tilde{M} \in [-20, 20]\ \text{GeV},\\
\text{mass mixing hierarchy factor,} &\quad \alpha \in [0.01, 1),\\
\text{scalar mass,} &\quad m_0 \in [100, 4000]\ \text{GeV},\\
\text{gaugino mass,} &\quad m_{1/2} \in [300, 4000]\ \text{GeV},\\
\text{soft mass mixing,} &\quad \tilde{m}^2 \in [-5\times 10^6, 5\times 10^6]\ \text{GeV}^2,\\
\text{trilinear coupling,} &\quad A_0 \in [-4000, 4000]\ \text{GeV},\\
\text{soft bilinear term VL fields,} &\quad B_0 \in [-1500, 1500]\ \text{GeV},\\
\text{ratio of the Higgs VEVs,} &\quad \tan\beta \in [1, 60],
\end{aligned}
$$

and the sign of the Higgs mass parameter, sgn $\mu = +1$.

The experimental constraints used to derive the parameter space in addition to the Higgs bounds are flavor physics constraints such as BR$(\bar{B} \to X_s\gamma)$ [78], BR$(B_u \to \tau\nu)$ [79], $\Delta M_{B_s}$ [80], $\Delta\rho$ [80], BR$(B_s \to \mu^+\mu^-)$ [81,82], and BR$(\tau^\pm \to \mu^\pm\gamma)$ [83], while in the DM sector the constraint on relic abundance [84], $\Omega_\chi h^2$, and the current LUX limit [85] on the spin-independent DM-nucleon scattering cross section, $\sigma_p^{\rm SI}$, are taken into account. For more details on ranges and theoretical and experimental errors see Table 1 of Ref. [32].

## IV. ALLOWED PARAMETER SPACE AND DECAY PROPERTIES OF EWINOS

In this section we study decay properties of $\chi_1^\pm$ and $\chi_2^0$ in the parameter space which satisfies the constraints mentioned in the previous section as well as $\delta(g-2)_\mu$ bounds

[2]The result shown in Fig. 1 is obtained using the same numerical tools and priors used in Ref. [32].

$(2\sigma)$ as shown in Fig. 1. The $2\sigma$ allowed region for $\delta(g-2)_\mu$ according to the latest data [1,2] is indicated by the blue solid lines, while the dashed lines indicate future measurement [3,4] with 4 times greater sensitivity, assuming that the central value remains the same. We consider the red points that are allowed by current $\delta(g-2)_\mu$ bounds for further analysis. The trilepton final states from direct chargino-neutralino pair production will be the most effective channel to probe all these points. Because of the choice of input parameters and mixing in our model, it is expected that the decay modes of EWinos could be different from the MSSM cases or usual choices made by ATLAS/CMS with simplified scenarios.

### A. Decay modes for $\chi_2^0$

In general for light slepton scenarios (lighter than $m_{\chi_1^\pm}$), the second lightest neutralino $\chi_2^0$ decays into two body final state—$l\tilde{l}$ and $\nu\tilde{\nu}$ where $l$ denotes $e$, $\mu$, and $\tau$. For our model, the first slepton mass eigenstate is mostly mixed smuon/VL, and the second slepton eigenstate is usually right-handed stau. Hence we sometimes obtain large mass splitting between the first two slepton mass eigenstates. For a significant portion of the parameter space $\chi_2^0$ decays to a muon and a slepton at 50% branching ratio, or one sees the $\tau$ lepton channel but no electrons, with 50% branching ratio for invisible modes. Thus the flavor democratic simplified model scenarios are mostly absent in our model. As a result, apart from the invisible modes which have a 50% branching ratio, $\chi_2^0$ can dominantly decay into either $\mu\tilde{\mu}$ or $\tau\tilde{\tau}$ with 50% branching ratios. For the first case the usual LHC limit will then provide more stringent bounds.

In the left panel of Fig. 2, the branching ratios for different leptonic decay modes are plotted against the $\chi_2^0$ mass. The muon channel is always at 50% branching ratio but the $\tau$ channel has a branching ratio which is mostly less than 20% with some points having branching ratio in the range between 20% and 100% while no electrons are seen.

In Fig. 3, we present the branching ratios of $\chi_2^0$ which decays into a muon and a slepton $(\tilde{e}_1/\tilde{e}_2)$, where the slepton further decays into a muon and an LSP with 100% branching ratio. The points are color coded according to the mass differences $m_{\tilde{e}} - m_{\chi_1^0}$ (left panel) and $m_{\chi_2^0} - m_{\tilde{e}}$ (right panel). These BRs$(\chi_2^0 \to \mu\tilde{e}_{1/2} \to \mu\mu\chi_1^0)$ vary within 40%–50% with the rest being invisible, where the slepton could be degenerate with either $\chi_1^0$ or $\chi_2^0$.

### B. Decay modes for $\chi_1^\pm$

The charginos decay into $l\tilde{\nu}$ and $\nu\tilde{l}$ with equal branching ratios for three generations in the "flavor-democratic" simplified model. As we discussed in the previous subsection, because of the different smuon mixing as compared to MSSM, the charginos largely decay into $\nu\tilde{\mu}$ and $\mu\tilde{\nu}$ with a branching ratio of 50% each or the corresponding $\tau$ lepton channel.

In the right panel of Fig. 2, we show the branching ratios into different leptonic channels for $\chi_1^\pm$ as a function of $m_{\chi_1^\pm}$. We can see that the chargino dominantly decays to muons with a very small fraction going to $\tau$ and none to electrons. Thus a three muon signal is the most likely and also the most constraining signature to look for in the trilepton searches.

In Fig. 4, we present the branching ratios of $\chi_1^\pm$ where it decays into a neutrino and a slepton $(\tilde{e}_1/\tilde{e}_2)$, where the slepton further decays into a muon and an LSP. The points are color coded according to the mass differences $m_{\tilde{e}} - m_{\chi_1^0}$ (left panel) and $m_{\chi_1^\pm} - m_{\tilde{e}}$ (right panel). These BRs$(\chi_1^\pm \to \nu\tilde{e}_{1/2} \to \nu\mu\chi_1^0)$ vary within 40%–50% with the rest being $\chi_1^\pm \to \mu\tilde{\nu}$, where the slepton could be degenerate with either $\chi_1^0$ or $\chi_2^0$.

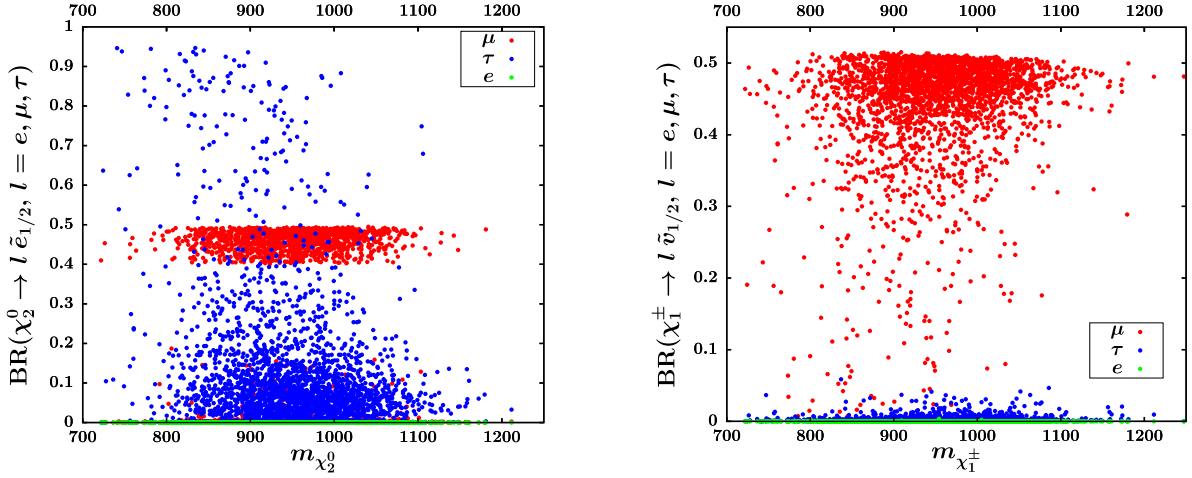


FIG. 2. Branching ratio of $\chi_2^0 \to l\tilde{e}$ (left panel) and $\chi_1^\pm \to l\tilde{\nu}$ (right panel) plotted against $\chi_2^0$ and $\chi_1^\pm$ masses, respectively, for the parameter space satisfying the constraints described in the text as well as giving a $(g-2)_\mu$ contribution that is within the current $2\sigma$ limit.

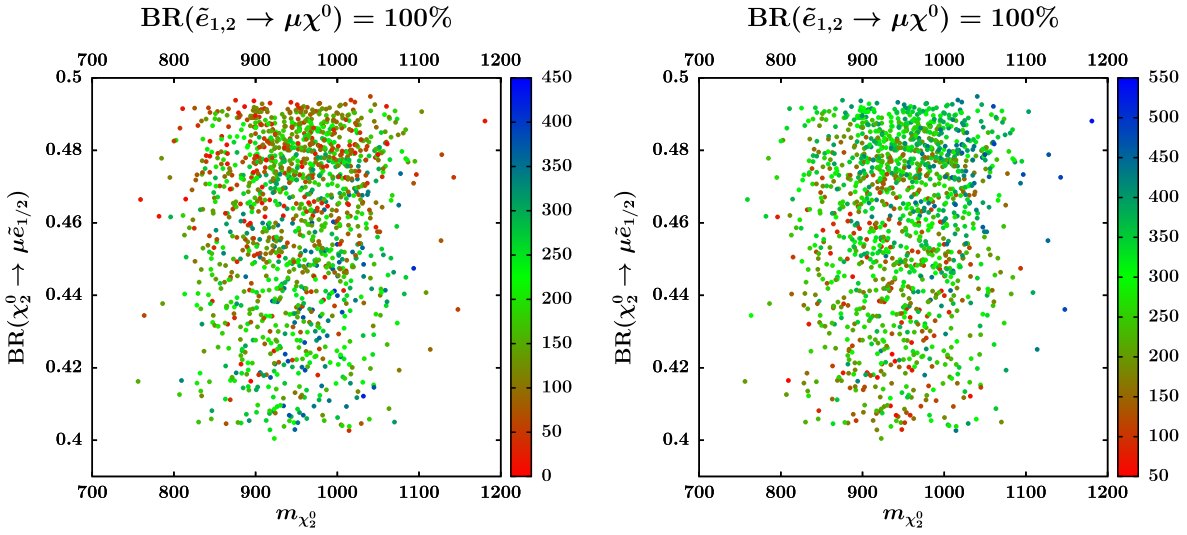


FIG. 3. Branching ratio of $\chi_2^0 \to \mu\tilde{e}$ plotted against $\chi_2^0$ mass for parameter space satisfying the constraints described in the text as well as giving a $(g-2)_\mu$ contribution that is within the current $2\sigma$ limit. The left panel shows the points color coded with slepton-LSP mass difference while the right panel shows them color coded according to the $\chi_2^0$-slepton mass difference.

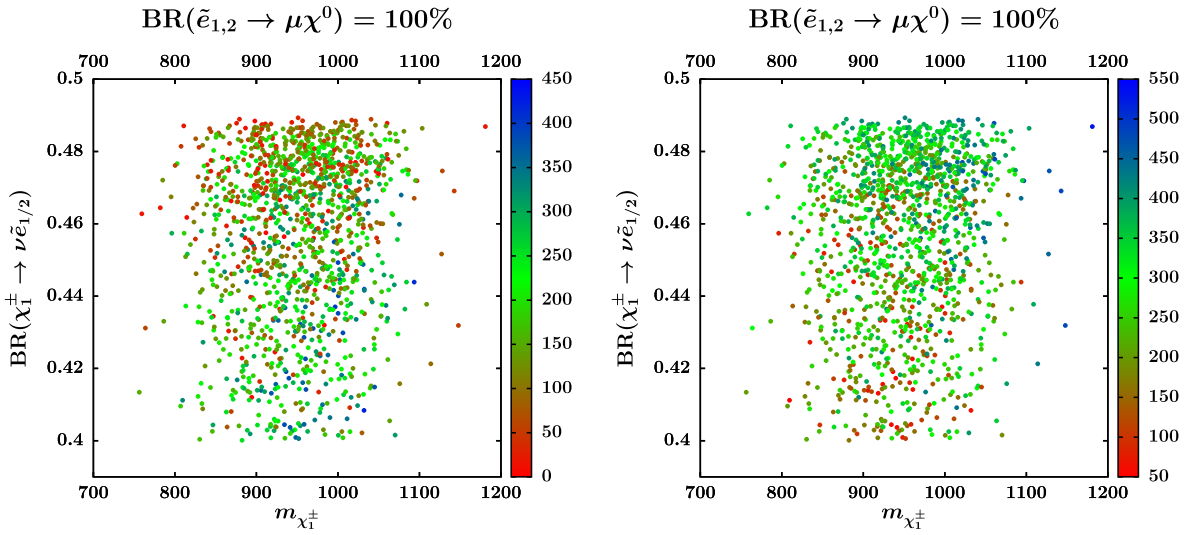


FIG. 4. Same as Fig. 3 but for $\chi_1^\pm \to \nu\tilde{e}$ with the points in the left panel color coded according to the mass difference $m_{\tilde{e}} - m_{\chi_1^0}$ while those in the right panel are according to $m_{\chi_1^\pm} - m_{\tilde{e}}$.

### C. Benchmark points and models

From the results of the previous section on the decay modes of $\chi_1^\pm$ and $\chi_2^0$, we can see that the collider constraint that is best suited to probe the chargino-neutralino pair production are the trilepton searches. In Table I, we show three benchmark points chosen from Figs. 2–4. The decay properties of these points are strikingly different from the usual simplified models considered by LHC Collaboration to interpret the trilepton limits. Also the mass hierarchies between sleptons and the electroweakinos are different in our model. Motivated by these benchmark points we choose the following three scenarios, or benchmark models:

(i) *Benchmark Model 1 (BM1)*: This model is motivated by benchmark point 1 (BP1) where the electroweakinos dominantly decay into muons. Here sleptons are next to lightest supersymmetric particle and nearly degenerate with the LSP, and we assume $m_{\tilde{\nu}_1} = m_{\tilde{e}_1} = m_{\chi_1^0} + 10$ GeV. For the branching ratios of the electroweakinos we assume $\mathrm{BR}(\chi_1^\pm \to \mu\tilde{\nu}_1, \nu\tilde{e}_1) = 0.50$ and $\mathrm{BR}(\chi_2^0 \to \mu\tilde{e}_1, \nu\tilde{\nu}) = 0.50$, where $\mathrm{BR}(\tilde{e}_1 \to \mu\chi_1^0) = 1.0$. These assumptions apply to each point in the parameter space.

(ii) *Benchmark Model 2 (BM2)*: BM2 is motivated by BP2, and the decay patterns of BM2 are the same as

TABLE I. Benchmark points chosen such that they satisfy the constraints as described in the text as well as giving a contribution to $(g-2)_\mu$ that is consistent with the current $2\sigma$ limit. All masses are in GeV.

| | Parameter | BP1 | BP2 | BP3 |
|---|---|---|---|---|
| *GUT inputs* | $m_0$ | 1023 | 1162 | 970 |
| | $m_{1/2}$ | 1398 | 1544 | 1358 |
| | $A_0$ | 36 | 1317 | 606 |
| | $M_V$ | 329 | 324 | 746 |
| | $B_0$ | 692 | −410 | 278 |
| | $\lambda_5$ | −0.16 | −0.14 | −0.16 |
| | $\tilde{m}^2(\times 10^6)$ | 1.6 | 1.9 | 1.6 |
| | $\tilde{M}$ | 4.3 | 4 | −10.9 |
| | $\tan\beta$ | 44.7 | 48.5 | 48.8 |
| | $\lambda_{D,2}$ | −0.39 | −0.34 | −0.38 |
| | $\lambda_{L,2}$ | −0.2 | −0.17 | −0.19 |
| *Pole masses* | $m_h$ | 124 | 123 | 123 |
| | $m_{\chi_1^0}$ | 474 | 526 | 463 |
| | $m_{\chi_1^\pm}$ | 898 | 993 | 875 |
| | $m_{\tilde{e}_1}$ | 484 | 576 | 669 |
| | $m_{\tilde{e}_2}$ | 858 | 866 | 752 |
| | $m_{\tilde{\nu}_1}$ | 475 | 569 | 663 |
| | $m_{\tilde{t}_R}$ | 2021 | 2297 | 1986 |
| *Branching ratios* | $\chi_1^\pm \to \mu\tilde{\nu}$ | 0.5 | 0.5 | 0.5 |
| | $\chi_1^\pm \to \nu\tilde{e}_1$ | 0.49 | 0.48 | 0.47 |
| | $\chi_2^0 \to \mu\tilde{e}_1$ | 0.49 | 0.49 | 0.48 |
| | $\chi_2^0 \to \nu\tilde{\nu}$ | 0.5 | 0.5 | 0.49 |
| | $\tilde{e}_1 \to \mu\chi_1^0$ | 1.0 | 1.0 | 1.0 |
| | $\delta(g-2)_\mu(\times 10^{-9})$ | 2.54 | 2.23 | 2.09 |
| | $\Delta m = m_{\tilde{e}_1} - m_{\chi_1^0}$ | 10 | 50 | $(m_{\chi_2^0} - m_{\chi_1^0})/2$ |

BM1 but with the choice $m_{\tilde{\nu}_1} = m_{\tilde{e}_1} = m_{\chi_1^0} + 50$ GeV. This choice of mass dependence can significantly change the limits on chargino masses.

(iii) *Benchmark Model 3 (BM3)*: BM3 is motivated by BP3, and the decay patterns of chargino and neutralino are similar to previous benchmark models. We choose the slepton mass as $m_{\tilde{\nu}_1} = m_{\tilde{e}_1} = (m_{\chi_2^0} + m_{\chi_1^0})/2$. This choice of mass basically is similar to the simplified models considered by ATLAS, but BM3 is different in terms of branching ratios.

## V. COLLIDER ANALYSIS FOR TRILEPTON SEARCHES

Both CMS and ATLAS Collaborations have searched for the EWinos with different final states ($2l, 3l$, with/without $taus, lbb, l\gamma\gamma$, etc.) from direct pair production of $\chi_1^\pm\chi_2^0$ or $\chi_1^\pm\chi_1^\pm$ [39–47]. The results are mainly interpreted for *slepton mediated simplified model*, *WZ mediated simplified model*, and *Wh mediated simplified model*. In the first case, the sleptons are assumed to be lighter than $\chi_1^\pm$ and $\chi_2^0$, and this channel gives the most stringent bounds as the EWinos decay via slepton to lepton enriched final states [46]. For the rest of the two cases, sleptons are assumed to be much heavier than $\chi_1^\pm$ or $\chi_2^0$ and the electroweakinos decay via real or virtual $W$, $Z$, and Higgs boson. In our own model, the LHC limits on gluinos from 13 TeV data put stringent bounds on $m_{\chi_1^\pm} \gtrsim 700$ GeV (due to high scale input) and only the trilepton analysis targeting $\chi_1^\pm\chi_2^0$ production is sensitive to the $m_{\chi_1^\pm} > 700$ GeV region. Hence in this analysis we only focus on the trilepton channels (dedicated signal regions for slepton mediated simplified model). First we will briefly discuss the 13 TeV trilepton search analysis considered by ATLAS [46] and present our results alongside ATLAS for validation and direct comparison.

### A. Validation for trilepton analysis

In *slepton* $(\tilde{\ell}_L)$*-mediated* models, it is assumed that the left handed sleptons and sneutrinos lie exactly midway between $\chi_1^0$ and $\chi_2^0$, $m_{\tilde{\ell}_L} = (m_{\tilde{\chi}_1^\mp} + m_{\chi_2^0})/2$, and the EWinos decay either to left-handed sleptons or sneutrinos universally. Events are considered with exactly three tagged leptons (electron or muon) [46]. Event reconstruction details, such as electron, muon, tau and jet identification, isolation, and overlap removal, are followed according to the ATLAS analysis as mentioned in Secs. 5 and 6 of [46]. In this trilepton analysis, a veto on $b$-jet is applied to all signal channels. For $b$-jets, we use the $p_T$ dependent $b$-tagging efficiencies obtained by ATLAS Collaboration in Ref. [86].

Depending upon the requirement of $m_{\rm SFOS}$ [invariant mass of same-flavor opposite-sign (SFOS) lepton] and $p_T^{l_3}$ ($p_T$ of third leading lepton), ATLAS has optimized five signal regions (SR), namely, SR3$l$-a to SR3$l$-e for slepton mediated simplified model. The basic selection requirements for these channels, number of observed events, and total SM background are listed in Table II. In the absence of any BSM signal in all these channels, limits are set on the number of SUSY signal events at 95% confidence level (C.L.). For these five signal regions (SR3$l$-a to SR3$l$-e) $N_{\rm BSM}$ at 95% C.L. are 7.2, 5.5, 10.6, 3.0, and 3.0, respectively. The ATLAS Collaboration has translated these obtained upper limits on $N_{\rm BSM}$ into exclusion limits in the $m_{\chi_1^0}$-$m_{\chi_1^\pm}$ plane. In a similar way, we have also reproduced the exclusion contours obtained by ATLAS assuming similar mass relations and branching ratios of the relevant gauginos and sleptons. In order to validate our results we reproduce the exclusion contours using PYTHIA (v6.428) [87].[3] We use the next-to-leading order (NLO) + next-to-leading logarithmic (NLL) chargino-neutralino pair production cross sections given in Ref. [88], which have been calculated for 13 TeV using the RESUMMINO code [89,90]. For slepton mediated models, SR3$l$-e is the most sensitive

[3]These same setups of codes were also used in Ref. [59].

TABLE II. Selection requirements for slepton mediated ($3l$) channel considered by ATLAS for 13 TeV 36.1 fb$^{-1}$ data [46].

| | SR3$l$-a | SR3$l$-b | SR3$l$-c | SR3$l$-d | SR3$l$-e |
|---|---|---|---|---|---|
| $N_{\text{lepton}}$ | | | 3 | | |
| $\not{E}_T >$ (GeV) | | | 130 | | |
| $m_T^{\min} >$ (GeV) | | | 110 | | |
| $m_{\text{SFOS}}$ (GeV) | | <81.2 | | >101.2 | |
| $p_T^{l_3}$ (GeV) | 20–30 | >30 | 20–50 | 50–80 | >80 |
| Observed events | 4 | 3 | 9 | 0 | 0 |
| Total SM | $2.23 \pm 0.79$ | $2.79 \pm 0.43$ | $5.41 \pm 0.93$ | $1.42 \pm 0.38$ | $1.14 \pm 0.23$ |

channel for the parameter space with large mass splitting between $\chi_1^{\pm}$ and $\chi_1^0$ ($\delta m = m_{\chi_1^{\pm}} - m_{\chi_1^0}$). For smallest $\delta m$, low-valued $m_{\text{SFOS}}$ SR3$l$-a is more effective to probe the relevant parameter space.

In Fig. 5, we present the validated results for slepton mediated simplified models. The red line corresponds to 95% C.L. exclusion limits obtained by ATLAS, and the black line corresponds to our validated results adopting the ATLAS analysis. From Fig. 5, it is evident that our validated results are in good agreement with that of ATLAS.

### B. New limits for benchmark models

First we present our results for *Benchmark Model 1* (BM1), where the scenarios represent slepton coannihilation regions and due to the extreme mass degeneracy ($\delta m = m_{\chi_1^{\pm}} - m_{\chi_1^0} = 10$ GeV) the leptons coming from slepton decay are very soft (below the trigger cuts). The soft leptons cause the reduction on limits on chargino masses. The orange regions in Fig. 6 are excluded from 13 TeV data where the red dotted line represents the usual limits from simplified scenarios with the sleptons being midway between LSP and charginos. The vertical and horizontal magenta lines present the indirect limit on $m_{\chi_1^{\pm}}$ and $m_{\chi_1^0}$ from the gluino limits coming from 13 TeV data [91]. The blue points (circles) are allowed by the new muon $g-2$ result in a future measurement at Fermilab [3,4] while the red points (star) are ruled out, assuming that the central value of the measurement remains the same. It is clear from Fig. 6 that for coannihilation scenarios trilepton limits are even weaker than the indirect bounds from direct gluino searches due to the mass correlations in GUT models. It may be noted that with nonuniversal gaugino mass models the indirect limits from gluino searches are not valid and the models have a wide range of parameter space which is still allowed (except for the magenta regions).

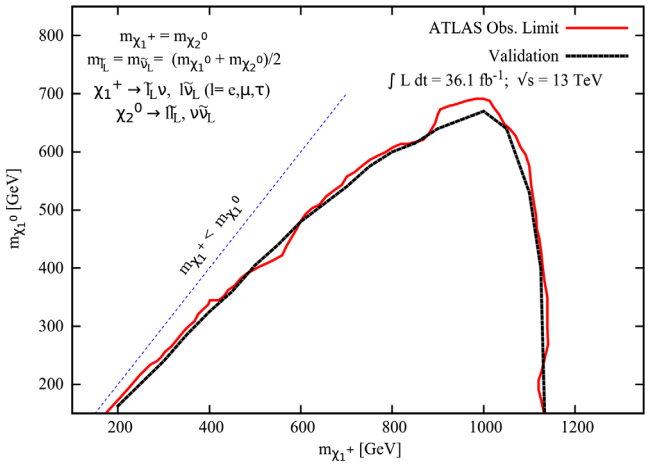


FIG. 5. Validation of the ATLAS trilepton analysis for Run-II 36.1 fb$^{-1}$ data [46]. The exclusion limit in the $m_{\chi_1^0} - m_{\chi_1^{\pm}}$ plane obtained by the ATLAS Collaboration (red line) in their trilepton analysis is reproduced using similar mass relations and branching ratios of the relevant gauginos and sleptons (black line).

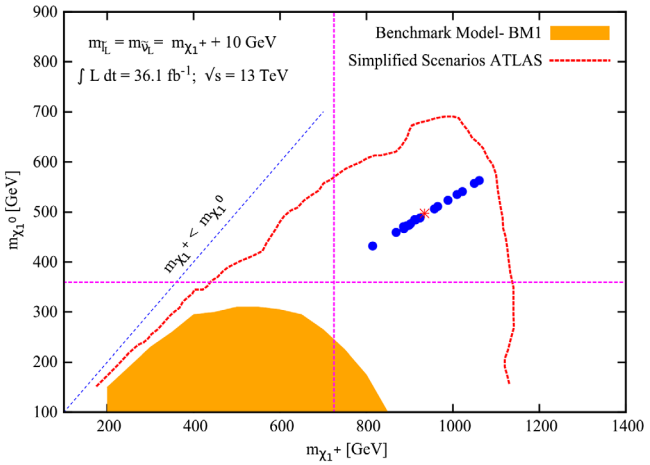


FIG. 6. Limits on $m_{\chi_1^{\pm}} - m_{\chi_1^0}$ plane for Benchmark Model 1 (see text). The excluded region for BM1 is shown in orange. The red dotted line represents the limit for slepton mediated simplified scenarios [46]. The magenta lines indicate the indirect lower limit on $m_{\chi_1^{\pm}}$ (vertical line) and $m_{\chi_1^0}$ (horizontal line) from gluino seaches in 13 TeV data [91]. The blue points (circles) will be allowed by the new muon $g-2$ result in a future measurement at Fermilab [3,4] while the red points (star) will be ruled out, assuming that the central value of the measurement remains the same.

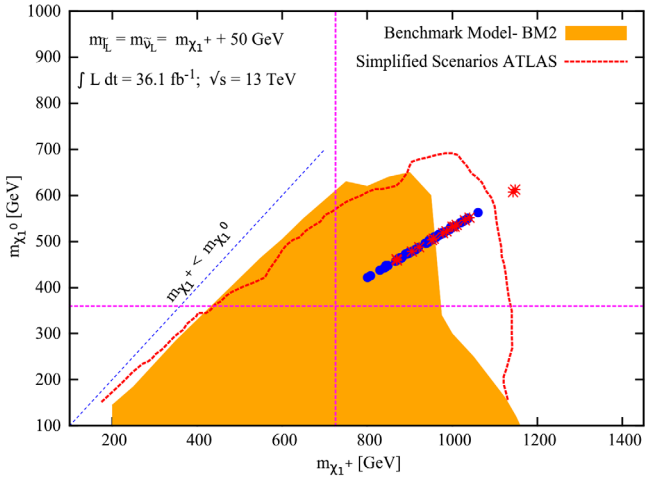


FIG. 7. Same as Fig. 6 but for Benchmark Model 2 (see text).

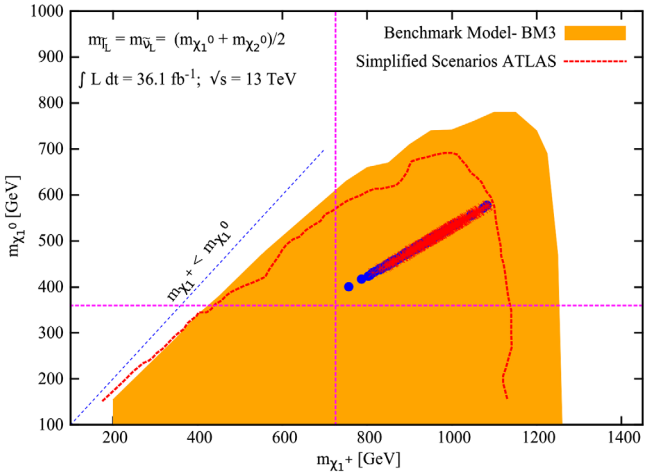


FIG. 8. Same as Fig. 6 but for Benchmark Model 3 (see text).

The situation changes drastically if the mass difference is somewhat larger. We present the implication of trilepton data in Fig. 7 for BM2 where the mass splitting between $\chi_1^{\pm}$ and $\chi_1^0$, $\delta m = m_{\chi_1^{\pm}} - m_{\chi_1^0}$, is 50 GeV. The orange regions in Fig. 7 are excluded for BM2. In some region of the parameter space the limits are stronger than usual simplified models (denoted by red line). This is simply due to the enhancement of branching ratios in our model. It may be noted that for the simplified models considered by ATLAS, the electroweakinos decay to leptonic final state universally (but for BM2, electroweakinos decay mainly to $\mu$ final states). In Fig. 7, roughly half the points outside the orange shaded region are ruled out by future muon $g-2$ experiment [3,4] as indicated by the red points.

In Fig. 8 we analyze the model BM3 where the sleptons are exactly midway of $\chi_1^{\pm}$ and $\chi_2^0$ (same choice as simplified models). Similar to BM1 and BM2, EWinos decay also mainly to $\mu$ final states in BM3. For this model, the limits are even stronger than BM2. For light $\chi_1^0$, the limit on chargino mass extends up to 1250 GeV. Hence the current LHC data exclude all the $(g-2)_\mu$ allowed points which have the same characteristic as BM3.

## VI. CONCLUSIONS

In this work we have studied the VL extension of MSSM—by the addition of a pair $\mathbf{5}+\bar{\mathbf{5}}$ of $SU(5)$ which leads to an additional quark, lepton, and a pair of neutrinos with corresponding squarks, sleptons, and sneutrinos—in the context of $(g-2)_\mu$, various flavor physics constraints, DM constraints, and LHC limits on squarks and gluinos. We identify that the allowed parameter space in Fig. 1 leads to chargino mass in the range of 700–1200 GeV. The mixing of the second and third generation leptons with the extended spectrum of VL particles leads not only to an enhanced contribution to $(g-2)_\mu$ but also gives a very different kind of signature for electroweakino decay modes.

To probe the allowed parameter space at the LHC, the most sensitive search will be the trilepton signal coming from chargino-neutralino pair production. For this reason we do a detailed study of relevant decay properties and the mass hierarchies in Secs. 4.1 and 4.2. In particular we observe that the VL extension of MSSM along with the specific choice of GUT scale parameters made here leads to a 3 muon or 3 tau final state instead of lepton universality assumed in the LHC trilepton analysis. We therefore recast the ATLAS trilepton searches in chargino-neutralino pair production using the recent Run-II data. We identify three benchmark points from the scanned data set. To interpret the trilepton search we construct three simplified benchmark models based on these benchmark points. We observe that the slepton coannihilation scenario, i.e., BM1, is not at all sensitive to the current LHC data due to the soft nature of the lepton signal (see Fig. 6). However, the points with a relatively larger mass difference, as for example BM2, can exclude chargino mass up to 1 TeV (see Fig. 7). The strongest constraint comes from BM3 where the slepton mass lies midway between the chargino and second lightest neutralino. For such a choice any parameter range allowed by $(g-2)_\mu$ data is already excluded (see Fig. 8). There still exists more than half of the parameter space that is not covered by the three benchmark models considered here, which were chosen such that they are most sensitive to the trilepton searches. For this parameter space, the allowed $2\sigma$ range of $\delta(g-2)_\mu$ from the new muon $g-2$ experiment at Fermilab [3,4] can potentially rule out more than two-thirds of the region, assuming that the central value of the $(g-2)_\mu$ measurement remains the same. Much of this parameter space consists of tau lepton final states in chargino-neutralino pair production, which is not sensitive to the current Run-II data with $\mathcal{L} = 36.1\ \text{fb}^{-1}$ [92]. Future searches with higher luminosity for $2\tau/3\tau$ signal at the LHC could potentially probe this region of the parameter space.

## ACKNOWLEDGMENTS

We thank Luc Darmé and Enrico Maria Sessolo for the useful discussions in the initial stage of this work. A. C. and S. R. thank Luc Darmé for helpful inputs to numerical computation. A. C. and L. R. are supported by the Lancaster-Manchester-Sheffield Consortium for Fundamental Physics under STFC Grant No. ST/L000520/1. S. R. and L. R. are supported in part by the National Science Council (NCN) research Grant No. 2015-18-A-ST2-00748. The use of the CIS computer cluster at the National Centre for Nuclear Research in Warsaw is gratefully acknowledged.

[1] G. W. Bennett *et al.* (Muon $g-2$ Collaboration), Final report of the muon E821 anomalous magnetic moment measurement at BNL, Phys. Rev. D **73**, 072003 (2006).
[2] J. P. Miller, E. de Rafael, and B. L. Roberts, Muon $g-2$: Experiment and theory, Rep. Prog. Phys. **70**, 795 (2007).
[3] J. Grange *et al.* (Muon $g-2$ Collaboration), Muon (g-2) technical design report, arXiv:1501.06858.
[4] A. Chapelain (Muon $g-2$ Collaboration), The Muon g-2 experiment at Fermilab, Eur. Phys. J. Web Conf. **137**, 08001 (2017).
[5] M. Endo, K. Hamaguchi, S. Iwamoto, and T. Yoshinaga, Muon $g-2$ vs LHC in Supersymmetric Models, J. High Energy Phys. 01 (2014) 123.
[6] A. Fowlie, K. Kowalska, L. Roszkowski, E. M. Sessolo, and Y.-L. S. Tsai, Dark matter and collider signatures of the MSSM, Phys. Rev. D **88**, 055012 (2013).
[7] M. Chakraborti, U. Chattopadhyay, A. Choudhury, A. Datta, and S. Poddar, The electroweak sector of the pMSSM in the light of LHC—8 TeV and other data, J. High Energy Phys. 07 (2014) 019.
[8] S. P. Das, M. Guchait, and D. P. Roy, Testing SUSY models for the muon g-2 anomaly via chargino-neutralino pair production at the LHC, Phys. Rev. D **90**, 055011 (2014).
[9] M. Chakraborti, U. Chattopadhyay, A. Choudhury, A. Datta, and S. Poddar, Reduced LHC constraints for higgsino-like heavier electroweakinos, J. High Energy Phys. 11 (2015) 050.
[10] M. Lindner, M. Platscher, and F. S. Queiroz, A call for new physics: The muon anomalous magnetic moment and lepton flavor violation, arXiv:1610.06587.
[11] M. Endo, K. Hamaguchi, S. Iwamoto, and K. Yanagi, Probing minimal SUSY scenarios in the light of muon $g-2$ and dark matter, J. High Energy Phys. 06 (2017) 031.
[12] A. Fowlie, M. Kazana, K. Kowalska, S. Munir, L. Roszkowski, E. M. Sessolo, S. Trojanowski, and Y.-L. S. Tsai, The CMSSM favoring new territories: The impact of new LHC limits and a 125 GeV Higgs, Phys. Rev. D **86**, 075010 (2012).
[13] P. Bechtle *et al.*, Killing the cMSSM softly, Eur. Phys. J. C **76**, 96 (2016).
[14] J. Cao, Z. Heng, D. Li, and J. M. Yang, Current experimental constraints on the lightest Higgs boson mass in the constrained MSSM, Phys. Lett. B **710**, 665 (2012).
[15] S. Mohanty, S. Rao, and D. P. Roy, Reconciling the muon $g-2$ and dark matter relic density with the LHC results in nonuniversal gaugino mass models, J. High Energy Phys. 09 (2013) 027.
[16] S. Akula and P. Nath, Gluino-driven radiative breaking, Higgs boson mass, muon g-2, and the Higgs diphoton decay in supergravity unification, Phys. Rev. D **87**, 115022 (2013).
[17] J. Chakrabortty, S. Mohanty, and S. Rao, Non-universal gaugino mass GUT models in the light of dark matter and LHC constraints, J. High Energy Phys. 02 (2014) 074.
[18] K. Kowalska, L. Roszkowski, E. M. Sessolo, and A. J. Williams, GUT-inspired SUSY and the muon $g-2$ anomaly: Prospects for LHC 14 TeV, J. High Energy Phys. 06 (2015) 020.
[19] J. Chakrabortty, A. Choudhury, and S. Mondal, Non-universal Gaugino mass models under the lamppost of muon (g-2), J. High Energy Phys. 07 (2015) 038.
[20] A. S. Belyaev, J. E. Camargo-Molina, S. F. King, D. J. Miller, A. P. Morais, and P. B. Schaefers, A to Z of the muon snomalous magnetic moment in the MSSM with Pati-Salam at the GUT scale, J. High Energy Phys. 06 (2016) 142.
[21] N. Okada and H. M. Tran, 125 GeV Higgs boson mass and muon $g-2$ in 5D MSSM, Phys. Rev. D **94**, 075016 (2016).
[22] T. Fukuyama, N. Okada, and H. M. Tran, Sparticle spectroscopy of the minimal SO(10) model, Phys. Lett. B **767**, 295 (2017).
[23] M. Endo, K. Hamaguchi, S. Iwamoto, and N. Yokozaki, Higgs mass, muon $g-2$, and LHC prospects in gauge mediation models with vector-like matters, Phys. Rev. D **85**, 095012 (2012).
[24] M. Endo, K. Hamaguchi, S. Iwamoto, and N. Yokozaki, Higgs mass and muon anomalous magnetic moment in supersymmetric models with vector-like matters, Phys. Rev. D **84**, 075017 (2011).
[25] R. Dermisek and A. Raval, Explanation of the Muon g-2 anomaly with vectorlike leptons and its implications for Higgs decays, Phys. Rev. D **88**, 013017 (2013).
[26] R. Dermisek, A. Raval, and S. Shin, Effects of vectorlike leptons on $h \to 4\ell$ and the connection to the muon g-2 anomaly, Phys. Rev. D **90**, 034023 (2014).
[27] I. Gogoladze, Q. Shafi, and C. S. Un, Reconciling the muon g-2, a 125 GeV Higgs boson, and dark matter in gauge mediation models, Phys. Rev. D **92**, 115014 (2015).
[28] A. Aboubrahim, T. Ibrahim, and P. Nath, Leptonic $g-2$ moments, *CP* phases and the Higgs boson mass constraint, Phys. Rev. D **94**, 015032 (2016).
[29] M. Nishida and K. Yoshioka, Higgs boson mass and muon g-2 with strongly coupled vector-like generations, Phys. Rev. D **94**, 095022 (2016).

[30] T. Higaki, M. Nishida, and N. Takeda, Flavor structure, Higgs boson mass and dark matter in supersymmetric model with vector-like generations, Prog. Theor. Exp. Phys. **2017**, 083B04 (2017).
[31] E. Megias, M. Quiros, and L. Salas, $g_\mu - 2$ from vector-like leptons in warped space, J. High Energy Phys. 05 (2017) 016.
[32] A. Choudhury, L. Darmé, L. Roszkowski, E. M. Sessolo, and S. Trojanowski, Muon g-2 and related phenomenology in constrained vector-like extensions of the MSSM, J. High Energy Phys. 05 (2017) 072.
[33] P. W. Graham, A. Ismail, S. Rajendran, and P. Saraswat, A little solution to the little hierarchy problem: A vector-like generation, Phys. Rev. D **81**, 055016 (2010).
[34] S. P. Martin, Extra vector-like matter and the lightest Higgs scalar boson mass in low-energy supersymmetry, Phys. Rev. D **81**, 035004 (2010).
[35] C. Faroughy and K. Grizzard, Raising the Higgs mass in supersymmetry with $t - t'$ mixing, Phys. Rev. D **90**, 035024 (2014).
[36] Z. Lalak, M. Lewicki, and J. D. Wells, Higgs boson mass and high-luminosity LHC probes of supersymmetry with vectorlike top quark, Phys. Rev. D **91**, 095022 (2015).
[37] K. Nickel and F. Staub, Precise determination of the Higgs mass in supersymmetric models with vectorlike tops and the impact on naturalness in minimal GMSB, J. High Energy Phys. 07 (2015) 139.
[38] R. Barbieri, D. Buttazzo, L. J. Hall, and D. Marzocca, Higgs mass and unified gauge coupling in the NMSSM with vector matter, J. High Energy Phys. 07 (2016) 067.
[39] G. Aad *et al.* (ATLAS Collaboration), Search for direct production of charginos and neutralinos in events with three leptons and missing transverse momentum in $\sqrt{s} = 8$ TeV $pp$ collisions with the ATLAS detector, J. High Energy Phys. 04 (2014) 169.
[40] G. Aad *et al.* (ATLAS Collaboration), Search for direct production of charginos, neutralinos and sleptons in final states with two leptons and missing transverse momentum in $pp$ collisions at $\sqrt{s} = 8$ TeV with the ATLAS detector, J. High Energy Phys. 05 (2014) 071.
[41] G. Aad *et al.* (ATLAS Collaboration), Search for the direct production of charginos, neutralinos and staus in final states with at least two hadronically decaying taus and missing transverse momentum in $pp$ collisions at $\sqrt{s} =$ 8 TeV with the ATLAS detector, J. High Energy Phys. 10 (2014) 096.
[42] G. Aad *et al.* (ATLAS Collaboration), Search for direct pair production of a chargino and a neutralino decaying to the 125 GeV Higgs boson in $\sqrt{s} = 8$ TeV $pp$ collisions with the ATLAS detector, Eur. Phys. J. C **75**, 208 (2015).
[43] G. Aad *et al.* (ATLAS Collaboration), Search for the electroweak production of supersymmetric particles in $\sqrt{s} = 8$ TeV $pp$ collisions with the ATLAS detector, Phys. Rev. D **93**, 052002 (2016).
[44] V. Khachatryan *et al.* (CMS Collaboration), Searches for electroweak neutralino and chargino production in channels with Higgs, Z, and W bosons in $pp$ collisions at 8 TeV, Phys. Rev. D **90**, 092007 (2014).
[45] V. Khachatryan *et al.* (CMS Collaboration), Searches for electroweak production of charginos, neutralinos, and sleptons decaying to leptons and W, Z, and Higgs bosons in $pp$ collisions at 8 TeV, Eur. Phys. J. C **74**, 3036 (2014).
[46] ATLAS Collaboration, Technical Report No. ATLAS-CONF-2017-039, CERN, Geneva, 2017.
[47] CMS Collaboration, Technical Report No. CMS-PAS-SUS-17-004, CERN, Geneva, 2017.
[48] A. Bharucha, S. Heinemeyer, and F. von der Pahlen, Direct chargino-neutralino production at the LHC: Interpreting the exclusion limits in the complex MSSM, Eur. Phys. J. C **73**, 2629 (2013).
[49] K. Howe and P. Saraswat, Excess Higgs production in neutralino decays, J. High Energy Phys. 10 (2012) 065.
[50] P. Schwaller and J. Zurita, Compressed electroweakino spectra at the LHC, J. High Energy Phys. 03 (2014) 060.
[51] D. Ghosh, M. Guchait, and D. Sengupta, Higgs signal in chargino-neutralino production at the LHC, Eur. Phys. J. C **72**, 2141 (2012).
[52] J. Eckel, M. J. Ramsey-Musolf, W. Shepherd, and S. Su, Impact of LSP character on slepton reach at the LHC, J. High Energy Phys. 11 (2014) 117.
[53] A. Choudhury and A. Datta, Neutralino dark matter confronted by the LHC constraints on electroweak SUSY signals, J. High Energy Phys. 09 (2013) 119.
[54] C. Han, L. Wu, J. M. Yang, M. Zhang, and Y. Zhang, New approach for detecting a compressed bino/wino at the LHC, Phys. Rev. D **91**, 055030 (2015).
[55] F. Yu, Anatomizing exotic production of the Higgs boson, Phys. Rev. D **90**, 015009 (2014).
[56] A. Papaefstathiou, K. Sakurai, and M. Takeuchi, Higgs boson to di-tau channel in chargino-neutralino searches at the LHC, J. High Energy Phys. 08 (2014) 176.
[57] M. A. Ajaib, B. Dutta, T. Ghosh, I. Gogoladze, and Q. Shafi, Neutralinos and sleptons at the LHC in light of muon $(g-2)_\mu$, Phys. Rev. D **92**, 075033 (2015).
[58] T. Han, S. Padhi, and S. Su, Electroweakinos in the light of the Higgs boson, Phys. Rev. D **88**, 115010 (2013).
[59] A. Choudhury and S. Mondal, Revisiting the exclusion limits from direct chargino-neutralino production at the LHC, Phys. Rev. D **94**, 055024 (2016).
[60] Q.-F. Xiang, X.-J. Bi, P.-F. Yin, and Z.-H. Yu, Searching for singlino-Higgsino dark matter in the NMSSM, Phys. Rev. D **94**, 055031 (2016).
[61] A. Datta, N. Ganguly, and S. Poddar, New limits on heavier electroweakinos and their LHC signatures, Phys. Lett. B **763**, 213 (2016).
[62] K. Hagiwara, K. Ma, and S. Mukhopadhyay, Closing in on the chargino contribution to the muon g-2 in the MSSM: Current LHC constraints, arXiv:1706.09313.
[63] A. Arbey, M. Boudaud, F. Mahmoudi, and G. Robbins, Robustness of dark matter constraints and interplay with collider searches for new physics, arXiv:1707.00426.
[64] M. Chakraborti, A. Datta, N. Ganguly, and S. Poddar, Multilepton signals of heavier electroweakinos at the LHC, arXiv:1707.04410.
[65] J. Cao, Y. He, L. Shang, W. Su, and Y. Zhang, Testing the light dark matter scenario of the MSSM at the LHC, J. High Energy Phys. 03 (2016) 207.
[66] A. Kobakhidze, M. Talia, and L. Wu, Probing the MSSM explanation of the muon g-2 anomaly in dark matter

experiments and at a 100 TeV $pp$ collider, Phys. Rev. D **95**, 055023 (2017).
[67] F. Feroz, M. P. Hobson, and M. Bridges, MultiNest: An efficient and robust Bayesian inference tool for cosmology and particle physics, Mon. Not. R. Astron. Soc. **398**, 1601 (2009).
[68] F. Staub, SARAH 4: A tool for (not only SUSY) model builders, Comput. Phys. Commun. **185**, 1773 (2014).
[69] F. Staub, Automatic calculation of supersymmetric renormalization group equations and self energies, Comput. Phys. Commun. **182**, 808 (2011).
[70] W. Porod and F. Staub, SPheno 3.1: Extensions including flavour, $CP$-phases and models beyond the MSSM, Comput. Phys. Commun. **183**, 2458 (2012).
[71] F. Staub, T. Ohl, W. Porod, and C. Speckner, A tool box for implementing supersymmetric models, Comput. Phys. Commun. **183**, 2165 (2012).
[72] W. Porod, F. Staub, and A. Vicente, A flavor kit for BSM models, Eur. Phys. J. C **74**, 2992 (2014).
[73] G. Belanger, F. Boudjema, A. Pukhov, and A. Semenov, micrOMEGAs$_3$: A program for calculating dark matter observables, Comput. Phys. Commun. **185**, 960 (2014).
[74] P. Bechtle, S. Heinemeyer, O. Stl, T. Stefaniak, and G. Weiglein, HiggsSignals: Confronting arbitrary Higgs sectors with measurements at the Tevatron and the LHC, Eur. Phys. J. C **74**, 2711 (2014).
[75] P. Bechtle, O. Brein, S. Heinemeyer, G. Weiglein, and K. E. Williams, HiggsBounds: Confronting arbitrary Higgs sectors with exclusion bounds from LEP and the Tevatron, Comput. Phys. Commun. **181**, 138 (2010).
[76] P. Bechtle, O. Brein, S. Heinemeyer, G. Weiglein, and K. E. Williams, HiggsBounds 2.0.0: Confronting neutral and charged Higgs sector predictions with exclusion bounds from LEP and the tevatron, Comput. Phys. Commun. **182**, 2605 (2011).
[77] P. Bechtle, O. Brein, S. Heinemeyer, O. Stl, T. Stefaniak, G. Weiglein, and K. E. Williams, HiggsBounds-4: Improved tests of extended Higgs sectors against exclusion bounds from LEP, the Tevatron and the LHC, Eur. Phys. J. C **74**, 2693 (2014).
[78] Y. Amhis *et al.*, Averages of $b$-hadron, $c$-hadron, and $\tau$-lepton properties as of summer 2016, arXiv:1612.07233.
[79] I. Adachi *et al.* (Belle Collaboration), Evidence for $B^- \to \tau^- \bar{\nu}_\tau$ with a Hadronic Tagging Method Using the Full Data Sample of Belle, Phys. Rev. Lett. **110**, 131801 (2013).
[80] C. Patrignani *et al.* (Particle Data Group), Review of particle physics, Chin. Phys. C **40**, 100001 (2016).
[81] R. Aaij *et al.* (LHCb Collaboration), Measurement of the $B_s^0 \to \mu^+\mu^-$ Branching Fraction and Search for $B^0 \to \mu^+\mu^-$ Decays at the LHCb Experiment, Phys. Rev. Lett. **111**, 101805 (2013).
[82] S. Chatrchyan *et al.* (CMS Collaboration), Measurement of the $B_s^0 \to \mu^+\mu^-$ Branching Fraction and Search for $B^0 \to \mu^+\mu^-$ with the CMS Experiment, Phys. Rev. Lett. **111**, 101804 (2013).
[83] B. Aubert *et al.* (*BABAR* Collaboration), Searches for Lepton Flavor Violation in the Decays $\tau^\pm \to e^\pm\gamma$ and $\tau^\pm \to \mu^\pm\gamma$, Phys. Rev. Lett. **104**, 021802 (2010).
[84] P. A. R. Ade *et al.* (Planck Collaboration), Planck 2015 results. XIII. Cosmological parameters, Astron. Astrophys. **594**, A13 (2016).
[85] D. S. Akerib *et al.* (LUX Collaboration), Results from a Search for Dark Matter in the Complete LUX Exposure, Phys. Rev. Lett. **118**, 021303 (2017).
[86] ATLAS Collaboration, Technical Report No. ATLAS-CONF-2012-043, CERN, Geneva, 2012.
[87] T. Sjostrand, S. Mrenna, and P. Z. Skands, PYTHIA 6.4 physics and manual, J. High Energy Phys. 05 (2006) 026.
[88] https://twiki.cern.ch/twiki/bin/view/LHCPhysics/SUSYCrossSections.
[89] B. Fuks, M. Klasen, D. R. Lamprea, and M. Rothering, Gaugino production in proton-proton collisions at a center-of-mass energy of 8 TeV, J. High Energy Phys. 10 (2012) 081.
[90] B. Fuks, M. Klasen, D. R. Lamprea, and M. Rothering, Precision predictions for electroweak superpartner production at hadron colliders with Resummino, Eur. Phys. J. C **73**, 2480 (2013).
[91] ATLAS Collaboration, Technical Report No. ATLAS-CONF-2017-022, CERN, Geneva, 2017.
[92] ATLAS Collaboration, Technical Report No. ATLAS-CONF-2017-035, CERN, Geneva, 2017.